

7401
74

AUG 5 1938



Library L. M. A. L.

TECHNICAL MEMORANDUMS
NATIONAL ADVISORY COMMITTEE FOR AERONAUTICS

No. 871

PERFORMANCE OF ROTATING-WING AIRCRAFT

By K. Hohenemser

Ingenieur-Archiv, Vol. 8, December 1937

To be returned
the file of the
Memorial
Laboratory

Washington
July 1938



3 1178 01440 3522

NATIONAL ADVISORY COMMITTEE FOR AERONAUTICS

TECHNICAL MEMORANDUM NO. 871

PERFORMANCE OF ROTATING-WING AIRCRAFT*

By K. Hohenemser

I. INTRODUCTION

A large amount of both theoretical and experimental information published lately has been devoted to the performance of rotating-wing aircraft. The term "rotating-wing aircraft," in the narrower sense, is limited hereinafter to aircraft whose gross weight is taken up by one or more rotors with a generally vertical axis. For these the patent literature has adopted the term "Steilschrauben" (autogiro rotors) to differentiate them from the eventually existent regular propellers.

Among the rotating-wing aircraft we differentiate the limiting cases of the helicopter with mechanically driven, forward-tilted autogiro rotors and no regular propellers ("helicopter" in English literature, "gyroplane," according to Bréguet), and the autogiro fitted with regular propeller (autogiro) on which there is no mechanical drive of the backward-tilted, windmill-like operating autogiro rotor in flight. Between these two extremes lies the "Flugschrauber" (a term coined by Th. Mohring (reference 1)), or "Helicogyro" (according to V. Isacco (reference 2)), with both the regular propellers and the autogiro rotors driven mechanically. Depending upon the power distributed over the regular propeller and the autogiro rotors, a helicogyro can fly in the helicopter or in the autogiro stage.

A wealth of information on autogiro problems is found in the reports of J. B. Wheatley, who improved and extended the investigations started by H. Glauert (reference 3), and subsequently continued by C. N. H. Lock (reference 4). Wheatley has explored the problem of rotor blades hinged to the rotor axis (Cierva) theoretically (reference 5) in the wind tunnel (reference 6) and in free-flight tests (reference 7). Just as exhaustively did he investigate the Risseler-Wilford rotor, on which each two opposite

*"Zur Frage der Flugleistungen von Drehflüglern." Ingenieur-Archiv, vol. 8, December 1937, pp. 433-449.

blades are rigidly mounted and jointly able to oscillate freely about the longitudinal axis of the blade (reference 8). Concerning their aerodynamic quality, the rotors are practically equivalent, and wind-tunnel tests with the rotors in autorotating condition and rectangular blades and a solidity (or ratio of total-blade area to swept-disk area) of $\sigma = 0.1$, give minimum lift/drag ratios of 1/5 to 1/6 which, with smaller solidity and for the characteristic values of full-scale design can be lowered to 1/8-1/9.* In addition, the calculations by L. Bréguet (reference 9), V. Isacco (reference 2, loc.cit.), H. G. Kussner (reference 10), H. H. Platt (reference 11), and H. B. Squire (reference 12), have shown some very promising performances for rotating-wing aircraft in isolated cases. But up to the present there has been no coordinated presentation from which the influence of the constants essential for the performance of rotating-wing aircraft could be obtained in systematic manner, nor has there been a comparison with the few available test data. The attempt at such a survey is to be made in the following, whereby nonessential factors, such as effect of blade form, blade profile, blade number, and blade twist on the performances are disregarded. Even the torsional flexibility of the blades is overlooked, although in practice it is very essential for the blade incidence. This omission is justified, according to J. A. Deavan and C. N. H. Lock (reference 13), who showed that the torsional flexibility of the blades has scarcely any influence on the efficiency of the rotor.

II. THE FLOW THROUGH THE SWEEPED-DISK AREA OF THE ROTOR

The assumption that the induced rate of downwash on the rotor is constant over the disk area represents, to be sure, an optimum condition for the energy loss, but even so, the posed assumption affords satisfactory estimates of the performance loss in cases where the optimum condition is not complied with, similar to the airfoil theory. Let

*J. de la Cierva indicated 1/13 to 1/14 as optimum values for the lift/drag ratio of autogiros, exclusive of hub resistance (Luftwissen No. 2, 1935, p. 113), but it is not quite clear whether the results were obtained by theory or by experiment.

α denote the angle of attack of the plane of rotor disk to the direction of flow (fig. 1). The air force S is approximately perpendicular to the plane of the rotor disk, hence the induced rate of downwash is assumed to be perpendicular to the plane of the rotor disk. Suppose it is v_{d1} at the blade, or $2v_{d1}$ at infinity, while the flow velocity at infinity (flying speed) is v . Then the resultant velocity at the rotor is

$$\sqrt{(v - v_{d1} \sin \alpha)^2 + v_{d1}^2 \cos^2 \alpha}$$

We resort to a formula originating with H. Glauert (reference 3), according to which the thrust S is equal to twice the product of swept-disk area F , air density ρ , induced downward velocity at the point of the rotor v_{d1} , and the resultant velocity at the point of the rotor

$$S = F \rho 2v_{d1} \sqrt{(v - v_{d1} \sin \alpha)^2 + v_{d1}^2 \cos^2 \alpha} \quad (1)$$

This formula has never been proved correct except for vertical and for approximately horizontal flow through the swept-disk area, while in the intermediate zone it presents an unproved interpolation. However, this element of doubt as to the validity of equation (1) in the intermediate zone does not concern us since we shall confine ourselves in the disposition of the ultimate result to the cited limiting cases. Equation (1) follows, according to H. G. Küssner (reference 10), from the momentum theorem if the air mass participating in the momentum creation is made to equal the quantity of flow through a sphere circumscribing the rotor.

For small rotor angle of attack α , and small thrust factors c_s (disregarding v_{d1}^2/v^2 in relation to 1), equation (1) gives:

$$\frac{S}{F \frac{\rho}{2} v^2} = c_s = 4 \frac{v_{d1}}{v} \quad (2)$$

that is, a relation expressing Prandtl's airfoil theory for a circular airfoil, and which was proved approximately valid for propellers also (reference 14). For $\alpha = -90^\circ$, i. e., for vertical ascent, it gives:

$$\frac{S}{F \frac{\rho}{2} v^2} = c_s = 4 \left(1 + \frac{v_{d1}}{v}\right) \frac{v_{d1}}{v} \quad (3)$$

or an equation of the simple propeller slipstream theory. Figure 2 shows the thrust c_s plotted against v_{d1}/v for different α in logarithmic scale.

The rate of flow v_d through the plane of the rotor disk is, according to figure 1:

$$v_d = v_{d1} - v \sin \alpha$$

for small α , according to equation (2):

$$v_d = c_s \frac{v}{4} - \alpha v$$

and for $\alpha = -90^\circ$, according to equation (3):

$$v_d = \frac{v}{2} (1 + \sqrt{1 + c_s})$$

The introduction of the coefficient of advance $\lambda = \frac{v}{u}$ and of the thrust coefficient $k_s = \lambda^2 c_s = S/(F \frac{\rho}{2} u^2)$ referred to the tip speed u of the blade tips, gives for the coefficient of axial flow $\lambda_d = v_d/u$, the equations

$$\lambda_d = \frac{k_s}{4\lambda} - \alpha \lambda \quad (4)$$

applicable at small α and great λ and

$$\lambda_d = \frac{\lambda}{2} + \frac{1}{2} \sqrt{\lambda^2 + k_s} \quad (5)$$

valid for $\alpha = -90^\circ$.

The angle of attack α in equation (4) will be considered small as long as the sine is exchangeable with the arc, and the cosine is approximately 1; that is, up to about $\pm 15^\circ$. The condition of great λ in equation (4) is necessary because c_s was assumed small in equation (2). For the thrust coefficients k_s encountered in practice, equation (4) affords ample approximations at $\lambda > 0.1$.

High rates of climb in vertical ascent must be foregone in the dimensioning of high-speed rotative-wing aircraft as will be shown. So, except in special cases, λ^2 in

equation (5) may be neglected against k_s , which leaves

$$\lambda_d = \frac{\lambda}{2} + \frac{1}{2}\sqrt{k_s} \quad (6)$$

valid for $\alpha = -90^\circ$ and $\lambda^2 \ll k_s$.

The corresponding equation, generalized - that is, for any α , reads:

$$\frac{k_s^2}{16} = (\lambda_d + \lambda \sin \alpha)^4 \left[1 + \frac{1}{\left(\frac{\lambda_d}{\lambda} + \sin \alpha\right)^2} - \frac{2 \sin \alpha}{\frac{\lambda_d}{\lambda} + \sin \alpha} \right] \quad (7)$$

III. AERODYNAMIC FORCES ON THE ROTOR

The following equations established by H. Glauert (reference 15) are applicable to a rotor with rectangular untwisted blades which execute a periodic rotatory motion about the longitudinal blade axis, so that the rolling and pitching moments of the rotor disappear. As proved by G. H. H. Lock (reference 4), the equations are also approximately valid for a rotor with hinged blades, provided the blades are heavy enough. Then, however, angle α must be referred to the plane of the tip disk area, whose normal for the rotor with hinged blades in flight does not coincide with the true axis of rotation. The slope of the straight lift line for the blade section is assumed at $c_a' = 6.0$. It was computed with a profile drag coefficient c_w independent of the profile angle of attack. The thrust decrease toward the blade tips, which depends upon blade number and blade loading, is not allowed for. A further inaccuracy is introduced by the invalidity of the initial differential equations in the regions in which the air strikes the blade elements from the rear. Still the integration result is little affected by it so long as the coefficients of advance remain moderate. The dynamic pressure of a blade element was applied with the velocity component in the plane of the rotor and perpendicular to the blade axis. That is, the radial velocity component is neglected and the rate of flow through the plane of the rotor is assumed to be small in relation to the tip speed.

The equations for the blade-setting angle ϕ , referred to zero lift line, for the thrust coefficient k_s , for the

effective torque $k_d = \frac{(75 \eta_G \Pi_{St})}{\left(F \frac{\rho}{2} u^3\right)}$, where $\eta_G \Pi_{St}$ is the

performance on the rotor hub in horsepower, and for the coefficient of the rearward force normal to the rotor axis

$k_{sn} = \frac{R_n}{\left(F \frac{\rho}{2} u^3\right)}$, where R_n is the rearward force normal

to the rotor axis, in relation to the coefficient of advance in the plane of the rotor λ' , to the coefficient of axial flow λ_d , to the mean blade incidence ϕ_0 , to the solidity σ , and to the mean profile drag coefficient c_w read as follows:

$$\phi = \phi_0 - \phi_1 \sin \psi \quad (8)$$

$$\phi_1 = \frac{\frac{3}{2} \phi_0 \lambda' - 2 \lambda' \lambda_d}{1 + \frac{3}{2} \lambda'^2} \quad (9)$$

$$k_s = 2\sigma \left[\phi_0 \left(1 + \frac{3}{2} \lambda'^2\right) - \frac{3}{2} \lambda_d - \frac{3}{2} \lambda' \phi_1 \right] \quad (10)$$

$$k_d = 2\sigma \left[\frac{c_w}{8} (1 + \lambda'^2) + \lambda_d \left(\phi_0 - \frac{3}{2} \lambda_d - \frac{3}{4} \lambda' \phi_1\right) \right] \quad (11)$$

$$k_{sn} = 2\sigma \left[\lambda' \left(\frac{c_w}{4} + \frac{3}{2} \phi_0 \lambda_d\right) - \frac{3}{4} \phi_1 \lambda_d \right] \quad (12)$$

The azimuth angle ψ is measured from the rearward setting of the blade in direction of the rotation. The two special cases $\alpha = -90^\circ$ and small α lead to particularly simple equations and will be considered only. For $\alpha = -90^\circ$, the inflow velocity in the plane of the rotor disappears and with it λ' in equations (9) to (12), leaving $\phi_1 = 0$, $k_{sn} = 0$, and

$$k_s = 2\sigma \left(\phi_0 - \frac{3}{2} \lambda_d\right) \quad \text{valid for } \alpha = -90^\circ \quad (13)$$

$$k_d = \sigma \frac{c_w}{4} + \lambda_d 2\sigma \left(\phi_0 - \frac{3}{2} \lambda_d\right) = \sigma \frac{c_w}{4} + k_s \lambda_d$$

valid for $\alpha = -90^\circ$ (14)

The coefficient of axial flow λ_d dependent on k_s and λ follows from equation (5) or (6). In the conversion of the air force coefficients to the wind axis system of coordinates, equation (10) remains approximately unchanged for small α , while the interference coefficient

$$k_{sh} = \frac{R_h}{\left(\frac{\rho}{2} u^2 \right)} \quad (R_h \text{ being the resultant force component}$$

along the flight path (directed to the rear) follows as

$$k_{sh} = k_{sn} + \alpha k_s$$

Equations (9) to (12) are substantially simplified if

$$\delta_1 = 2\delta_0 \lambda' \quad (15)$$

is substituted for equation (9), which presents a good approximation for equation (9) at medium λ , in view of the assumedly small coefficient of axial flow λ_d . Then we obtain for small α , where the coefficient of advance λ' in the plane of the rotor can still be equated to the coefficient of advance λ in flight direction, the following equations which, in consideration of the omissions and inaccuracies in the derivation of Glauert's equations may raise objections, represent the true conditions - at least, as good as those:

$$\frac{k_s}{2\sigma} = \delta_0 \left(1 - \frac{3}{2} \lambda^2 \right) - \frac{3}{2} \lambda_d, \quad \text{valid for small } \alpha \quad (-15^\circ < \alpha < +15^\circ) \quad (16)$$

$$\frac{k_d}{2\sigma} = \frac{c_w}{8} (1 + \lambda^2) + \lambda_d \frac{k_s}{2\sigma}, \quad \text{valid for small } \alpha \quad (-15^\circ < \alpha < +15^\circ) \quad (17)$$

$$\frac{k_{sh}}{2\sigma} = \lambda \frac{c_w}{4} + \alpha \frac{k_s}{2\sigma}, \quad \text{valid for small } \alpha \quad (-15^\circ < \alpha < +15^\circ) \quad (18)$$

λ_d is taken from equation (4).

Within the cited limits for α , we find practically every flight condition of rotating-wing aircraft: level flight, climb and glide with moderate angle of climb and glide, the autogiro stage with backward-tilted rotor axis, the helicopter stage with rotor axis tilted forward, and the intermediate stages of the helicogyro. For hovering and vertical ascent, the respective equations (5), (6),

(13), and (14) are applicable. For the determination of the sinking speed in vertical descent ($\alpha = 90^\circ$) with power off, a rotor drag coefficient of $c_w St = 1.3$ can be assumed.

Then the air-force coefficients can be computed if the geometric constants ϕ_0 and σ , the profile drag c_w and the constants λ and α for the flight condition are given. The equations are most conveniently solved if k_g and λ are given, because then λ_d can be computed from equation (16), and α from equation (4), so that all terms on the right-hand side of equations (17) and (18) are known.

IV. QUALITY OF ROTATING-WING AIRCRAFT

As criterion for the quality of an airplane in high-speed flight, the factor* used is

$$\eta_s = \frac{v G}{270 N} \quad (19)$$

wherein G = gross weight in kilograms, v the flying speed in kilometers per hour, and N = horsepower. The airplane is then particularly well suited for high speed if, with given flying speed v , the factor η_s and consequently, the power loading G/N is as great as possible. For the fixed-wing aircraft in horizontal flight, the equation

$$\eta_s = \eta_z \frac{c_a}{c_{wg}} \quad (20)$$

is applicable, where η_z = propeller efficiency, c_a = lift coefficient, and c_{wg} = total drag coefficient.

As criterion for the quality in climbing, the factor*

$$\eta_{St} = \frac{1}{37.5} \frac{G}{N} \sqrt{\frac{P_0}{\rho}} \sqrt{\frac{G}{F}} \quad (21)$$

is used, where G = gross weight, F = wing or swept-disk

*This is the well-known figure of merit which, on fixed-wing aircraft, follows as the product of the reciprocal glide coefficient with the propeller efficiency.

** η_{St} is so chosen that for ideal propeller of vanishing blade friction ($c_w = 0$) in hovering ($\lambda = 0$ in equations (5) and (14)), it assumes the value 1.

area, Π = horsepower, and ρ_0 = air density at sea level. The airplane is particularly suited for climbing if, with given wing loading G/F , the factor η_{St} , and consequently, the power loading G/Π is as great as possible, thus assuring a large reserve of climb. The equation for fixed-wing aircraft in horizontal flight is:

$$\eta_{St} = \frac{c_a^{3/2} \eta_Z}{2c_{wg}} \quad (22)$$

Now the corresponding equations are to be derived for the rotating-wing aircraft, and under the assumption that the airplane has a regular propeller and part of the engine output is carried into the propeller. The total drag coefficient of the rotating-wing aircraft is $k_{sh} + \varphi \sigma \lambda^2$. Thereby $\varphi \sigma F$ is the equivalent parasite area of the nonlifting parts of the aircraft; or, in other words, φ indicates the ratio of equivalent parasite area to blade area. Since the whole drag must be overcome by the regular propeller, its share of the power is:

$$\Pi_Z = \frac{k_{sh} + \varphi \sigma \lambda^2}{\eta_Z} \frac{\rho}{2} u^2 F v$$

The performance quota of the autogiro rotor is:

$$\Pi_{St} = \frac{k_d}{\eta_G} \frac{\rho}{2} u^2 F u$$

with an assumed mechanical gear efficiency of η_G . Designating the ratio of autogiro rotor performance to total performance with ν gives for this ratio the equation:

$$\frac{\Pi_{St}}{\Pi_Z + \Pi_{St}} = \nu = \frac{1}{1 + \frac{\eta_G \lambda}{\eta_Z k_d} (k_{sh} + \varphi \sigma \lambda^2)} \quad (23)$$

The value for the high-speed factor η_S is, according to equation (19):

$$\eta_S = \frac{k_s \lambda}{k_d} \nu \eta_G = \frac{k_s \lambda \eta_G}{k_d + \frac{\eta_G}{\eta_Z} \lambda (k_{sh} + \varphi \sigma \lambda^2)} \quad (24)$$

and for the speed-of-climb factor η_{St} , according to equation (21):

$$\eta_{St} = \frac{k_s^{3/8}}{2k_d} v \eta_G = \frac{0.5 k_s^{3/8} \eta_G}{k_d + \frac{\eta_G}{\eta_Z} \lambda (k_{sh} + \varphi \sigma \lambda^2)} \quad (25)$$

Comparing equation (24) with equation (25) gives:

$$\eta_{St} = \frac{\eta_S \sqrt{k_s}}{2\lambda} \quad (26)$$

Now, assuming $\eta_Z = \eta_G$, the insertion of equations (4), (17), and (18) into equation (24) gives the equation:

$$\eta_S = \frac{\eta_G \frac{k_s}{2\sigma}}{\frac{c_W}{8} \left(3\lambda + \frac{1}{\lambda} \right) + \left(\frac{k_s}{2\sigma} \right)^2 \frac{\sigma}{2\lambda^2} + \varphi \frac{\lambda^2}{2}} \quad (27)$$

in which the rotor angle of attack α or, what is the same, the helicogyro constant v , is no longer present. η_{St} is given through equation (26). Assuming the mechanical efficiency of the power transfer to the autogyro rotor to be equal to the aerodynamic efficiency of the power conversion in the regular propeller, the high-speed and climbing factors of a rotating-wing aircraft are not dependent upon whether its stage is that of a helicopter with rotor tilted forward, or of an autogyro with backward-tilted autorotating rotor, or of an intermediate helicogyro stage. The departures from this theorem, based upon the assumed constancy of profile drag c_W with blade incidence, are discussed in section VIII.

Equation (27) is also readily obtainable from a consideration of the energy loss according to H. Glauert (reference 3). With $z =$ blade number, $t =$ blade chord, $r =$ distance of a blade element from the rotor center, and $R =$ rotor radius, the blade friction energy for small coefficient of axial flow and small rotor-blade angle, is approximately:

$$N_R = \frac{\rho}{2} u^3 z t \frac{c_W}{2\pi} \int_0^{2\pi} \int_0^R \left(\lambda \sin \psi + \frac{r}{R} \right) dr d\psi$$

Here the stream velocity in blade axis direction is disregarded and the integrand in the stage of backward inflow - that is, within the disk $\frac{1}{R} = -\lambda \sin \psi$ is inserted with wrong sign. But we could also (as, for instance, in Wheatley's reports) carry out the integration in the regions for forward and backward inflow separately and with different mean drag coefficients, but we shall concede the same omissions as in equations (8) to (12), and so confine ourselves to medium coefficients of advance.

Inserting the solidity $\sigma = \pi t / \pi R$, the integration gives:

$$\frac{N_R}{v} = \frac{\rho}{2} u^2 F \sigma \frac{C_W}{4} \left(3\lambda + \frac{1}{\lambda} \right)$$

The energy of momentum creation is $N_1 = S v_{d1}$ or with equation (2)

$$\frac{N_1}{v} = \frac{\rho}{2} u^2 F \frac{k_B^2}{4\lambda^2}$$

The resistance energy of the parasite residual resistance is

$$N_W = v \frac{\rho}{2} F u^2 \lambda^2 \varphi \sigma$$

Accordingly, the total performance N (in kg/s) required for horizontal flight is:

$$\frac{N}{v} = \frac{\rho}{2} u^2 F \left[\frac{\sigma C_W}{4} \left(3\lambda + \frac{1}{\lambda} \right) + \frac{k_B^2}{4\lambda^2} + \varphi \sigma \lambda^2 \right] \quad (28)$$

which, written in equation (19) with $G = S = k_B \frac{\rho}{2} F u^2$ and with consideration of the dimensions of N and v up to factor η_G stipulated in equation (19), gives equation (27) which, with the cited assumptions and limitations, is applicable to any rotor angle of attack α , and any blade angle of attack ϕ .

While equations (27) and (28) lose their validity at small coefficients of advance, equation (28) can also be employed at any other low-flying speed, according to Kussner (reference 10), by substituting the speed at the point of the rotor for the flying speed v , and forming

the coefficient of advance with the speed at the rotor. There is little difference if the flying speeds are high, because then the induced velocity is small relative to the flying speed. In the hovering stage v_d and λ_d substitute for v and λ in equation (28). By disregarding λ_d^2 relative to 1.0 and considering equation (5), equation (28) is identical with equation (14), which proves the correctness of equation (28) in the new meaning of the signs for both vanishing and higher flying speed. According to Küssner, the parentheses of equation (28) contain the term $(4\lambda + 1/\lambda)$ instead of $(3\lambda + 1/\lambda)$. Küssner's value is approximately reached at high flying speeds if the flow velocity in direction of the blade axes is taken into consideration; it is approximately reached at zero flying speed if the velocity perpendicular to the plane of the rotor is considered. In the latter case the difference is negligible because of the small coefficient of axial flow. Even at higher coefficients of advance the difference remains within the scope of accuracy of the present theory. The omitted radial velocities in equation (28) can, moreover, be justified as a certain allowance for c_w reduction of the blade profile in yaw.

In the following, equations (27) and (28) are used in their original form—that is, with v = flying speed, λ = coefficient of advance, and $\lambda > 0.1$ = limit of validity. The case of $\lambda = 0$ is treated separately. The total result then differs very little from that obtained with Küssner's performance formula.

V. HOVERING AND VERTICAL ASCENT

For $\alpha = -90^\circ$ and $\lambda = 0$, we have $k_g = 4\lambda_d^2$, according to equation (6), and $k_d = \frac{\sigma c_w}{4} + 4\lambda_d^3$, according to equation (14). The climbing factor for hovering is, according to equation (25):

$$\eta_{St} = \frac{k_g^{3/2}}{2k_d} = \frac{1}{1 + \frac{c_w}{5.66\sqrt{\sigma} \left(\frac{k_g}{2\sigma}\right)^{3/2}}} \quad (29)$$

The quantity $k_s/2\sigma$ is a measure for the aerodynamic blade loading. The choice of this quantity, with given rotor dimensions - that is, the selection of the rotative speed, is governed by various factors. If a rotating-wing aircraft is to show particularly good slow speeds, the climbing factor η_{st} , which rises with $k_s/2\sigma$, according to equation (29), is decisive. In reality, η_{st} reaches, as a result of separation of flow at the blades, a maximum at too high inflow angles, and drops again at still higher blade loadings. If the rotating-wing aircraft is to excel at high speed, the high-speed factor, according to equation (27), is decisive which reaches its maximum at substantially lower $k_s/2\sigma$, - to which should be added that, owing to the periodic rotations of the blades about the longitudinal axis for the purpose of equalizing the rolling and pitching moments at high speed, the air-stream angles for equal $k_s/2\sigma$ are in places substantially greater than in low-speed flight. In rotating-wing aircraft with coefficients of advance as high as $\lambda = 0.4$, the ratio $k_s/2\sigma$ should never exceed 0.1; in fact, it should be less than that for higher coefficients of advance. According to equation (29), it appears that the climbing factor increases unlimitedly with increasing solidity σ . But owing to the omitted thrust decrease at the blade tips which increases with the solidity, η_{st} reaches an optimum before very great solidity. For $k_s/2\sigma = 0.1$, this optimum should lie at $\sigma = 0.06$ to 0.08 . Figure 3 shows the climbing factor η_{st} for hovering, according to equation (29), against σ for $c_w = 0.016$ and $k_s/2\sigma = 0.09$. The thrust decrease at the blade tips has subsequently been corrected by a thrust reduction factor 0.9, and equation (29) was replaced by

$$\eta_{st} = \frac{0.85}{1 + \frac{c_w}{5.66 \sqrt{\sigma} \left(\frac{k_s}{1.8\sigma}\right)^{3/2}}} \quad (30)$$

A relation for vertical ascent is obtained by inserting equation (6) in equation (14):

$$k_d = \frac{\sigma c_w}{4} + k_s \frac{\lambda}{2} + \frac{k_s^{3/2}}{2}$$

In consequence, if k_{d0} denotes the effective torque for hovering $\lambda = 0$ and $k_s = \text{constant}$:

$$\text{or } \left. \begin{array}{l} k_d = k_{d0} + \frac{k_s \lambda}{2} \\ N = N_0 + \frac{Gv}{2} \end{array} \right\} \begin{array}{l} \text{valid for } \alpha = -90^\circ \\ \text{and } \lambda^3 \ll k_s \\ \\ \text{valid for } \alpha = -90^\circ \\ \text{and } \lambda^3 \ll k_s \end{array} \quad (31)$$

In vertical ascent, a helicopter with moderate climbing speed requires only half the power required for vertical ascent as excess over the power required for level flight. Compared to a fixed-wing aircraft, the helicopter requires in vertical ascent only half the climbing reserve.

VI. HORIZONTAL FLIGHT AND YAWING ASCENT

To illustrate the conditions in horizontal flight and in yawing ascent, equations (26) and (27) are evaluated in figure 4, whereby $c_w = 0.016$ and $\frac{k_s}{2\sigma} = 0.09$ as before, and the thrust decrease at the blade tips is allowed for by a subsequently applied thrust reduction factor of 0.9, so that equation (27) is replaced by

$$\eta_s = \frac{0.9 k_s / 1.8 \sigma}{\frac{c_w}{8} \left(3\lambda + \frac{1}{\lambda} \right) + \left(\frac{k_s}{1.8\sigma} \right)^2 \frac{\sigma}{2\lambda^3} + \varphi \frac{\lambda^3}{2}} \quad (32)$$

which contains the mechanical transmission efficiency or the propeller efficiency at $\eta_G = \eta_Z = 1$. The solidity is chosen at $\sigma = 0.05$. The curves are plotted for different ratios φ of equivalent parasite area to blade area. The highest horizontal speed is determined as follows: Determine η_{st} from the power loading G/N , the blade loading G/F , and the air-density ratio ρ_0/ρ , according to equation (21). The straight line $\eta_{st} = \text{constant}$ of figure 4, intersects the curve $\varphi = \text{constant}$ in the η_{st} diagram at one or two points. Transferring the points of intersection to the corresponding curve in the η_s chart gives, with the aid of

$$v = \frac{270 \eta_s}{G/\pi} \quad (33)$$

the maximum and minimum horizontal speed at full throttle, whereby the latter is zero if in our case $\eta_{st} < 0.60$. To obtain the highest possible speed for a given power loading G/H , the blade loading G/F must be so chosen that the intersection of the straight line $\eta_{st} = \text{constant}$ with the particular φ curve in the η_{st} chart lies exactly on the optimum of the corresponding φ curve in the η_s chart. Then, however, the speed range is very small; for $\varphi = 0.05$, for example, it amounts to 7:2. Since in the design of rotating-wing aircraft it is of particular importance to exploit the potentialities of a high speed range, it is necessary in our case to operate beyond the optimum high-speed factor. Lowering the minimum speed to zero by reducing the blade loading results for $\varphi = 0.05$ in a decrease of the maximum speed in the ratio of 7:6.3 as compared to the optimum. By an enlargement of the rotor equivalent to a mere 10-percent loss in maximum speed compared to the absolute optimum, the speed range is raised from 1:0.29 to 1:0. Here is where the most significant characteristic of the rotating-wing aircraft asserts itself.

The climbing performance is easily determined within the scope of validity of equation (32) - that is, down to $\lambda \approx 0.1$, because then the excess power available in horizontal flight is equal to the power required for vertical ascent. (It is presumed that in the calculation of η_{st} , according to equation (21), the transmission loss, or the propeller loss, respectively, is no longer contained in the performance N , since figure 4 is valid for $\eta_G = \eta_Z = 1$.) The approximate equivalence of power required for vertical ascent (gross weight times vertical climbing velocity) and the excessive thrust horsepower of the regular propellers relative to horizontal flight is, for fixed-wing aircraft and autogiros bound, as is known, only to the condition of moderate climbing angles. According to the dictum voiced in section IV, the sum of the performance of the autogiro rotor at the hub and of the thrust horsepower of the regular propeller at great coefficients of advance, is not affected by the flight condition, whether in helicopter, autogiro, or helicogyro stage. Consequently, the power required for vertical ascent, even of helicopters and helicogyros in climbing at moderate climbing angles is equal to the pure excess power (less transmission and propeller losses) compared to horizontal flight. This does not apply to climb at great angles, as shown in section V. If $\eta_{st \text{ max}}$ is the value of the climbing fac-

tor, according to figure 4 and η_{st} as obtained from equation (21) the equation for maximum rate of climb is

$$w = \frac{N\gamma_5}{G} \frac{\eta_{st \max} - \eta_{st}}{\eta_{st \max}} \quad (34)$$

(w in m/s, N in hp.). With $\eta_{st} = 0.6$ and $\varphi = 0.05$ in the above example, the obtained minimum speed was exactly zero. The climbing reserve at the speed of optimum climb then almost equals half the power required for level flight. The speed of best climb compared to a fixed-wing aircraft is low - here, 0.45 of the maximum speed. As a general rule, the rotating-wing aircraft with minimum speed = zero, possesses good climbing powers, while its speed of best climb is low.

The obtainment of climbing power in vertical ascent necessitates an enlargement of the rotor up to η_{st} values from less than 0.6 in our case. But as this means a further decrease in maximum speed, the rotating-wing aircraft, when used as high-speed craft, will have a moderate rate of climb in vertical ascent.

In flight at higher altitudes η_{st} increases with $\sqrt{\rho_0/\rho}$ and the speed range is accordingly quickly lowered

The rotating-wing aircraft retains the typical helicopter characteristics at low altitudes only, unless abnormally large rotors are used for high-speed flight.

The solidity effect σ is readily observed from equations (16), (26), and (32). For great λ , η_s is almost unaffected by σ , according to equation (32), while k_s increases with σ according to equation (16), and η_{st} with $\sqrt{\sigma}$ according to equation (26). By reducing the solidity, the left-hand curves of figure 4 would shift downward, and those on the right remain approximately the same. Reducing σ by 50 percent, for example, the intersection with the curve $\varphi = 0.05$ can, for $\eta_{st} = 0.6$, be brought to the point of optimum of the corresponding curve in the η_s diagram. The maximum speed would rise 10 percent, but the rate of climb would drop by more than 50 percent. Thus, solidities substantially less than 0.05 are impractical because they involve an abnormal drop in climbing power.

VII. COMPARISON WITH EXPERIMENTS

The most exhaustive wind-tunnel data on autogiro rotors available are those by J. B. Wheatley (reference 6). They are, to be sure, restricted to the autorotation stages, but equation (27) and figure 4 retain their validity for flight conditions with autorotation as well as for helicopter and helicogyro flight stages, hence the comparison with Wheatley's researches attains general significance.

Figure 5 shows the high-speed factor η_s for an autogiro rotor with N.A.C.A. section 4412, a solidity $\sigma = 0.1$ and an aerodynamic blade loading of $\frac{k_g}{2\sigma} = 0.072$ plotted against coefficient of advance λ (dashed curve) as compared with the result from equation (32) for $c_w = 0.016$. Up to $\lambda = 0.3$, the agreement with the calculation is good; beyond that figure the errors committed in the calculation, especially the omission of flow separation at large angles of attack, are noticeable. Since these processes are intimately associated with the Reynolds Number, it may be assumed that for the full scale the curve will approach the computed curve more closely, so that up to about $\lambda = 0.4$, the calculation should give acceptable values.

In figure 6 the high-speed factor η_s at $\lambda = 0.3$ is plotted for the same autogiro rotor against the aerodynamic blade loading $k_g/2\sigma$ (dashed curve) in comparison with the result of equation (32) for $c_w = 0.016$. At small blade loading the calculated drag coefficient c_w is, as is seen, too high; at higher $k_g/2\sigma$ too low, aside from the burbling phenomena which accompany it. In view of the pronounced schematization of the flow on the rotor effected in the theory, the result must suffice.

A further potential source of comparison is found in the wind-tunnel tests published by H. E. Platt (reference 11). His rotor blades, like Wheatley's, had rectangular tips and no twist; the solidity was $\sigma = 0.067$. His test points reduced to a residual parasite area per blade area ratio of $\phi = 0.06$ are included in figure 4. On making the comparison, it should be noted that the solidity was a little higher than 0.05, and the aerodynamic blade loading $k_g/2\sigma$, a little lower than 0.09, as assumed in the

mathematical curves of figure 4 - both influences which also, according to equation (32), vitiate the high-speed factor in relation to the curves shown in figure 4. In contrast to Wheatley's experiments in the autogiro stage, the tests here relate to the helicopter stage with the autogiro rotor axis tilted forward. Equation (32) therefore actually portrays experiments in the autogiro stage and experiments in the helicopter stage very satisfactorily.

The published experiments on propellers in yaw with zero or slight blade twist, are herewith exhausted, but a number of wind-tunnel measurements are available on the hovering stage and the stage of vertical ascent. Platt's autogiro rotor with rectangular blades of zero twist (reference 11) described above, has at around $k_g/2\sigma = 0.08$ a climbing factor in hovering, of $\eta_{st} = 0.62$, which agrees well with figures 3 and 4. A collection of Göttingen wind-tunnel tests on propellers of low pitch at the torque stand and at low λ is given in the report by O. Walchner (reference 16) along with the results of his calculations. His η_{st} values for hovering range between 0.69 and 0.74; the reason for the higher values compared to those by Platt, is the comparatively pronounced blade twist (pitch/diameter $\frac{H}{D} = 0.3$ to 0.5). That blades with such twist are very unfavorable in high-speed flight is proved by the experiments of O. Flachsbart and G. Kröber (reference 17). Such rotors are impractical for high-speed autogiros. Much information about the anticipated figures of merit η_{st} in the hovering stage is vouchsafed in G. Schoppe's compilation of flown helicopter performances (reference 18). The η_{st} values of the better helicopters, range - depending on twist - between 0.64 and 0.73 for single rotors, and 20 to 30 percent higher for superposed, oppositely rotating rotors.

VIII. HELICOPTER, HELICOGYRO, AND AUTOGIRO

For the plotting of the curves of figure 4, it was assumed that the efficiency of the regular propeller is equal to the mechanical efficiency of the transmission of power to the autogiro rotor. Only thus was it possible to set up generally applicable curves for helicopter, helicogyro, and autogiro. The efficiency of the regular propeller is usually inferior to the mechanical efficiency of

the power transmission to the autogiro rotor, so that the flight stages approaching the helicopter would be preferable to the stages approaching the autogiro. At high-speed flight, of course, the difference between helicopter and autogiro performance is not great, with propeller efficiencies around 0.8 and mechanical efficiencies of from 0.85 to 0.95. With its inferior propeller efficiency in climb, a helicopter will, in general, be substantially superior to the autogiro even with due allowance for the greater driving-gear weight of the helicopter.

Thus far it had been assumed that the component of the flow velocity perpendicular to the plane of the rotor v_d , had no effect on the flight performances, since the drag coefficient c_w of the blade elements was presumed to be independent of the angle of attack. In reality, the rate of axial flow and the blade twist must be so attuned to one another that for a given effective torque k_s the angles of attack of the blade elements and consequently, the drag coefficients of the blade elements are on an average as small as possible. The coefficient of axial flow λ_d for the helicopter stage follows from equation (17) with $k_d = 0$ at

$$\lambda_d = - \frac{c_w}{8} \frac{1 + \lambda^2}{k_s/2\sigma} \quad (35)$$

or with $c_w = 0.016$ and $k_s/2\sigma = 0.09$ as

$$\lambda_d = - 0.0222 (1 + \lambda^2) \quad (35a)$$

Consequently, so long as the coefficients of advance remain moderate, the coefficient of axial flow of the autogiro remains nearly unchanged.

The coefficient of axial flow for the autogiro follows from equations (18) and (4) with allowance for the term $\frac{\varphi\lambda^2}{2}$ to be written in (18) for the parasite residual drag with $k_{sh} = 0$ at

$$\lambda_d = \frac{\left(\frac{k_s}{2\sigma}\right)^2 \frac{\sigma}{2\lambda} + \frac{c_w}{4} \lambda^2 + \frac{\varphi\lambda^2}{2}}{k_s/2\sigma} \quad (36)$$

or with $c_w = 0.016$, $\frac{k_g}{2\sigma} = 0.09$, and $\sigma = 0.05$ at

$$\lambda_d = \frac{0.0045}{2} + 0.0444 \lambda^2 + 5.55 \varphi \lambda^3 \quad (36a)$$

For $\lambda = 0.4$ and $\varphi = 0.05$, it gives $\lambda_d = 0.0294$; for $\varphi = 0.1$, it is $\lambda_d = 0.0462$. In contrast to the autogyro, the helicopter therefore manifests a marked rise in coefficient of axial flow as the flying speed increases and a further rise in λ_d with increasing parasite residual resistance of the aircraft. For adaptation to the downward flow through the swept-disk area, a blade twist would be necessary. But as this narrows the limit of the autorotation range in the autogyro stage, reasons of safety in flight demand either zero or at the most only slightly twisted blades. With zero blade twist, an optimum value of the figure of merit can be expected for a given thrust coefficient k_g in a flight condition in which the plane of the rotor is approximately parallel to the direction of flight or, with consideration of the induced rate of downwash, is slightly positive in flight direction. Deviations toward the autogyro stage entail no substantial vitiation with respect to the optimum value, because the coefficient of axial flow is small in a suitably constructed autogyro, according to equation (35). But in the helicopter stage, especially at high-speed flight and with higher residual resistances as a result of the greater λ_d according to equation (36), a perceptibly poorer figure of merit must be looked for compared to the optimum value at vanishing axial flow.

To give an idea of the helicogyro stages in which the probable optimum of vanishing λ_d is attained, the power ratio v of the autogyro performance to total performance is computed according to equation (36), with k_d and k_{sh} inserted, according to equations (17) and (18), and α according to equation (4), all for $\lambda_d = 0$. Then, equating the gear ratio η_G to the propeller efficiency η_Z affords the equation:

$$v = \frac{1}{1 + \frac{8\lambda}{c_w (1 + \lambda^2)} \left(\lambda \frac{c_w}{4} + \frac{k_g}{2\sigma} \frac{k_g}{4\lambda^2} + \frac{\varphi \lambda^2}{2} \right)} \quad (37)$$

which in figure 7 (solid curve) is plotted for $\phi = 0.05$, $c_w = 0.016$, $\frac{k_a}{2\sigma} = 0.09$, and $\sigma = 0.05$. In the principal flight range v lies between 0.4 and 0.55; the autogyro rotor consumes only about 50 percent of the power.

A special type of helicogyro, suggested among others, by Oehnicheon (French patent No. 672670) consists in having the reaction torque of the rotor taken up by a regular propeller mounted laterally from the fuselage, which produces a thrust in the direction of flight. If a is the distance of the regular propeller axis from that of the rotor, and R the radius of the rotor, the assumption of $\eta_G = \eta_Z$ gives the readily derived equation:

$$v = \frac{1}{1 + \lambda \frac{R}{a}} \quad (38)$$

The corresponding curves for $\frac{a}{R} = 0.5$, and $\frac{a}{R} = 0.25$ have been included in figure 7 (dashed curves). The arrangement of a regular propeller at $1/4$ to $1/2$ of the rotor radius away from the rotor axis and the control of the thrust of this regular propeller so as to exactly balance the rotor torque, leads to an aircraft that operates over a wide flight range in the vicinity of the optimum at $\lambda_d = 0$. Since the propeller efficiency is substantially lower at low flight speeds, such an airplane is inferior in the low-speed range to a helicopter of the same wing loading.

The writer does not believe that there is any reason as yet to prefer this or that type of rotating-wing aircraft, as stated in so many reports on rotating-wing aircraft with varying results. The autogyro will be out of the competition if there is constructed a helicopter or helicogyro of equal reliability with moderately higher weight, as then the poorer flight performances of the autogyro at low-speed flight and climb could no longer be justified. Likewise, the appraisal of the other known types, counterrotating rotors side by side or one above the other, single-rotor type with torque balance through auxiliary propeller or auxiliary surfaces or with torque-free rotor drive through rotating propeller, combustion nozzles or flapping wings can only be given on the basis of natured designs. The following examples will give a brief survey of the practical potentialities of rotating-wing aircraft.

IX. EXAMPLES

The examples are based on the curves of figure 4: that is, rotor solidity $\sigma = 0.05$, and aerodynamic blade loading $\frac{k_B}{2\sigma} = 0.09$. The rotor speeds at high- and low-speed flight are identical. The maintenance of constant speed naturally requires control of the rotor-blade incidence, which is an obvious requirement for a helicopter and here is assumed for the autogire also. The flight performances can be somewhat improved if the speed can be changed in flight with the aid of a control gear, so that temporarily the optimum value is obtainable. As long as it does not involve the velocity of sound as limit, the flight performances can be improved by lowering the r.p.m. in low-speed flight relative to high speed because the mean blade angle of attack at which burbling takes place in spots, lies higher in low-speed flight at the lower periodic rotatory motions of the blade about the longitudinal axis. If the sound velocity enters as limit, the r.p.m. must be reduced in high-speed flight, because peripheral speed and flight speed at the advancing blade become additive. On flight performances we compute: the maximum speed, maximum speed of climb, speed of climb in vertical ascent, minimum speed with full throttle, and sinking speed in vertical descent ($\alpha_w = 1.3$), all for sea level. Given is the power loading G/N . The choice of blade loading depends upon whether more stress is laid upon slow-flight performances, including climb, or upon high speed. The choice of blade loading then decides the rotor tip speed also. The examples are computed for a single rotor or side-by-side rotor arrangement. The data with the exception of those for vertical ascent and descent, are approximately applicable also for superposed rotors of $\sigma = 0.025$ solidity each, if the blade loading is referred to the swept-disk area of one of the rotors.

For two rotors, one above the other in vertical ascent with around $\eta_{St} = 0.75$ instead of 0.60, can be figured.

a) Autogire resembling airplane, type C.30.— The curve $\varphi = 0.1$ of figure 4, serves as basis. The gross weight is $G = 850$ kg, the engine output $N = 140$ hp. The blade loading is assumed at 8.5 kg/m², giving a rotor diameter of $D = 11.3$ m; $n = 207$ r.p.m., and a tip speed

of $u = 123$ m/s. The propeller efficiency at top speed is $\eta_z = 0.75$. Then we have:

$$\eta_{st} = \frac{8.1 \sqrt{8.5}}{37.5} = 0.63$$

and, according to figure 4, a coefficient of advance of $\lambda = 0.4$, or a maximum speed of

$$v_{max} = 123 \times 0.4 \times 3.6 = 176 \text{ km/h}$$

Let $\eta_z = 0.60$ at the speed of optimum climb - that is, $\eta_{st} = 0.79$. According to figure 4, we have $\eta_{st \text{ max}} = 1.1$ for $\varphi = 0.1$; that is, the speed of climb, according to equation (34) is:

$$w_{max} = \frac{140 \times 0.6 \times 75}{850} \left(\frac{1.1 - 0.79}{1.1} \right) = 2.1 \text{ m/s}$$

At minimum speed with full throttle, let $\eta_z = 0.5$, or $\eta_{st} = 0.94$, and $\lambda = 0.11$, according to figure 4. Consequently, the minimum speed with full throttle is:

$$v_{min} = 123 \times 0.11 \times 3.6 = 49 \text{ km/h}$$

This speed is, in reality, higher, since the curves of figure 4 are no longer valid for the related high angles of attack of the rotor. For power off in vertical descent, it is:

$$w_{min} = - 10.2 \text{ m/s}$$

b) Helicopter of the same horsepower and loading.-

The increase in weight due to the driving gears is assumed at 170 kg, which brings the gross weight now to $G = 1,020$ kg. The blade loading remains the same, $\varphi = 0.1$; the rotor diameter is $D = 12.4$ m (or 8.7 m each for side-by-side rotors); the speed is $n = 190$ r.p.m.; the tip speed, $u = 123$ m/s ($n = 270$ r.p.m. for side-by-side rotors). The efficiency of the mechanical power transmission is $\eta_g = 0.9$. Then $\eta_{st} = 0.63$ as before, and the maximum speed is again

$$v_{max} = 176 \text{ km/h}$$

The speed of climb is:

$$v_{\max} = \frac{140 \times 0.9 \times 75}{1020} \left(\frac{1.1 - 0.63}{1.1} \right) = 4.0 \text{ m/s}$$

The minimum speed with full throttle is:

$$v_{\min} = 4.4 \text{ km/h}$$

The blade loading being the same, the maximum rate of descent is the same as before. Under the effected assumptions the change from autogiro to helicopter of the same horsepower and loading has left the maximum speed as before, while the speed of climb has become almost twice as high and the minimum speed reduced to 1/10. With two counterrotating rotors, one above the other, of 12.4 m diameter, a climbing power in vortical ascent of

$$w = \frac{140 \times 0.9 \times 75}{1020} \left(\frac{0.75 - 0.63}{0.75} \right) 2 = 3.0 \text{ m/s}$$

may be expected. (The factor 2 follows from equation 31.)

c. Helicopter similar to He 70 airplane.— The He 70 type has with $G = 3,300 \text{ kg}$ and $n = 630 \text{ hp.}$, a speed of 355 km/h at sea level. For the corresponding helicopter the same power loading and a blade loading of 20 kg/m^2 is assumed. Then the rotor diameter is $D = 14.5 \text{ m}$ (that of each rotor is $D = 10.2 \text{ m}$ if two rotors are mounted side by side), the speed is $n = 250 \text{ r.p.m.}$ (355 r.p.m. for two rotors side by side), and the tip speed is $u = 189 \text{ m/s}$. It gives:

$$\eta_{st} = \frac{5.23 \sqrt{20}}{37.5} = 0.63$$

On account of the propitious body form, the curve for $\omega = 0.05$ of figure 4 is being used. Then $\lambda = 0.485$ and

$$v_{\max} = 0.485 \times 189 \times 3.6 = 332 \text{ km/h}$$

The speed of climb is:

$$w_{\max} = \frac{630 \times 75}{3300} \left(\frac{1.17 - 0.63}{1.17} \right) = 6.6 \text{ m/s}$$

The minimum speed with full throttle is:

$$v_{\min} = 6.8 \text{ km/h}$$

The sinking speed in vertical descent is:

$$w_{\min} = 15.7 \text{ m/s}$$

For two counterrotating rotors, one above the other, of $D = 14.5 \text{ m}$, the climbing power in vertical ascent would be:

$$v = \frac{630 \times 75}{3300} \left(\frac{0.75 - 0.63}{0.75} \right)^2 = 4.6 \text{ m/s}$$

no allowance being made for eventual weight increases due to power-plant installation with framework, or mechanical losses. The comparison becomes further unfavorable for the rotating-wing aircraft if the cruising performances are involved, because then the flying speed decreases approximately proportionately to the engine power, while for the fixed-wing aircraft the flying speed drops only approximately as $\sqrt[3]{P}$. Besides, for various reasons, it is more difficult to reach similar low values of the parasite residual resistance of the fixed-wing aircraft. But even so, the rotating-wing aircraft does not show up unfavorably in comparison with a very efficient fixed-wing type.

Naturally, these data present only rough estimations. Bréguet, for instance, assumes for his 1940 helicopter project, an η_S curve, which is substantially more favorable than the curve $\varphi = 0.05$ of figure 4. According to him, his helicopter should at $\lambda = 0.8$, reach its maximum high-speed factor η_S , alleged to be almost 10. These figures are too favorable according to present data, although a more careful appraisal of the flight-performance possibilities of rotating-wing aircraft justifies the assumption that a logical development research on rotating-wing aircraft will produce types which for many purposes will be superior to the orthodox airplane. When appraising special types such as Fieseler's Storch Fi 156, it should not be overlooked that so far it has been impossible to raise the ratio of maximum/minimum speed of a fixed-wing aircraft beyond 5:1, so that the requirement of a minimum speed of, say, 40 km/h for the purpose of safe field landing fundamentally conditions the maintenance of an upper speed limit of 200 km/h, regardless of the engine power available. With a rotating-wing aircraft of the same or even lower minimum speed, the same engine power affords considerably higher maximum speed.

RECAPITULATION

Glauert's equations for the air forces on propellers in yaw with rectangular blade tips, and with rolling and pitching moment balance through periodic blade twist or flapping motion, are simplified through an approximate assumption and served in discussion of the special characteristics of helicopters, helicogyros, and autogyros. Formulas are developed for high-speed and climbing efficiency, in which the effects of power loading, blade loading, solidity, r.p.m., and parasite residual resistance on the performances of rotating-wing aircraft are readily observed.

Translation by J. Vanier,
National Advisory Committee
for Aeronautics.

REFERENCES

1. Mohring, Th.: Fragen des Drehflüglers. Luftwissen, vol. 3, no. 8, August 1936, pp. 208-214; and vol. 4, no. 1, January 1937, pp. 12-21.
 2. Isacco, V.: Modern Helicopter Theory. A Complete Exposition of Up-to-Date Ideas on the Principles of Direct Lift Flight. Aircraft Engineering, October 1936, pp. 274-283; and November 1936, pp. 303-8.
 3. Glauert, H.: A General Theory of the Autogyro. R. & M. 1111, British A.R.C., 1926.
 4. Lock, G. N. H.: Further Development of Autogyro Theory. Parts I and II. R. & M. No. 1127, British A.R.C., 1927.
 5. Wheatley, J. B.: An Aerodynamic Analysis of the Autogyro Rotor with a Comparison between Calculated and Experimental Results. T.R. No. 487, N.A.C.A., 1934.
- Wheatley, J. B.: A Study of Autogyro Rotor-Blade Oscillations in the Plane of the Rotor Disk. T.N. No. 581, N.A.C.A., 1936.

REFERENCES (Cont.)

6. Wheatley, J. B.: Wind-Tunnel Tests of 10-Foot-Diameter Autogiro Rotors. T.R. No. 552, N.A.C.A., 1936.
7. Wheatley, J. B.: Lift and Drag Characteristics and Gliding Performance of an Autogiro as Determined in Flight. T.R. No. 434, N.A.C.A., 1932.
Wheatley, J. B.: Wing Pressure Distribution and Rotor-Blade Motion of an Autogiro as Determined in Flight. T.R. No. 475, N.A.C.A., 1933.
Wheatley, J. B.: The Influence of Wing Setting on the Wing Load and Rotor Speed of a POA-2 Autogiro as Determined in Flight. T.R. No. 523, N.A.C.A., 1935.
8. Wheatley, J. B., and Bioletti, Carlton: Wind-Tunnel Tests of a 10-Foot-Diameter Gyroplane Rotor. T.R. No. 536, N.A.C.A., 1935.
Wheatley, J. B.: The Aerodynamic Analysis of the Gyroplane Rotating-Wing System. T.N. No. 492, N.A.C.A., 1934.
9. Bréguet, Louis: The Gyroplane - Its Principles and Its Possibilities. T.M. No. 816, N.A.C.A., 1937.
10. Küssner, H. G.: Helicopter Problems. T.M. No. 327, N.A.C.A., 1937.
11. Platt, H. H.: The Helicopter: Propulsion and Torque. Jour. of the Aeronautical Sciences, vol. 3, no. 11, September 1936, p. 398.
12. Squire, H. B.: The Flight of a Helicopter. R. & M. No. 1730, British A.R.C., 1935.
13. Beavan, J. A., and Lock, C. M. H.: The Effect of Blade Twist on the Characteristics of the C.30 Autogiro. R. & M. No. 1727, British A.R.C., 1936.
14. Schrenk, M.: Aerodynamic Principles of the Direct Lifting Propeller. T.M. No. 733, N.A.C.A., 1934.
15. Glauert, H.: On the Horizontal Flight of a Helicopter. R. & M. No. 1157, British A.R.C., 1928.
Durand, W. F.: Aerodynamic Theory. Julius Springer, Berlin, 1935, vol. IV, p. 318.

REFERENCES (Cont.)

- 16 Walchner, O.: Berechnung von Luftschrauben mit kleinem Schubbeiwert und kleinem Fortschrittsgrad (Hubschrauben), Luftfahrtforschung, vol. 13, no. 4, April 20, 1936, p. 103.
17. Flachsbart, O., and Kroeber, G.: Experimental Investigation of Aircraft Propellers Exposed to Oblique Air Currents. T.M. No. 562, N.A.C.A., 1930.
18. Schoppe, G.: Der Bau von Hubschraubern seit 1900. Luftwissen, vol. 3, no. 5, May 1936, p. 127.

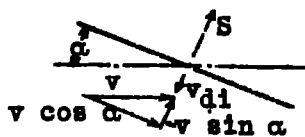


Figure 1.- Velocity distribution along the rotor.

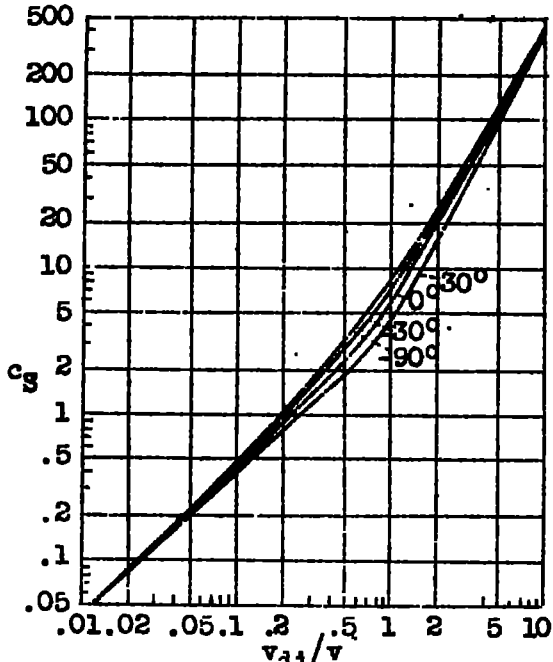


Figure 2.-Thrust factor against angle of attack and induced velocity.

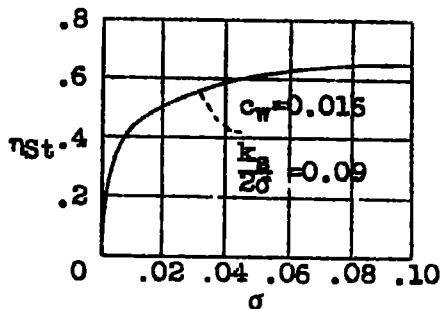


Figure 3.-Climbing factor against solidity according to eq. (30).

Figure 4.- Climbing and high-speed factor against coefficient of advance and parasite residual drag.

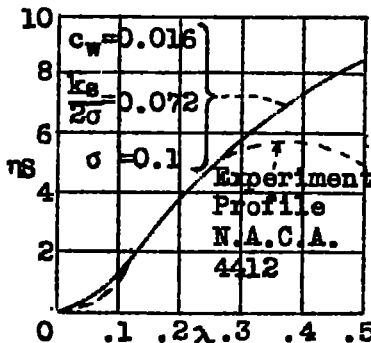
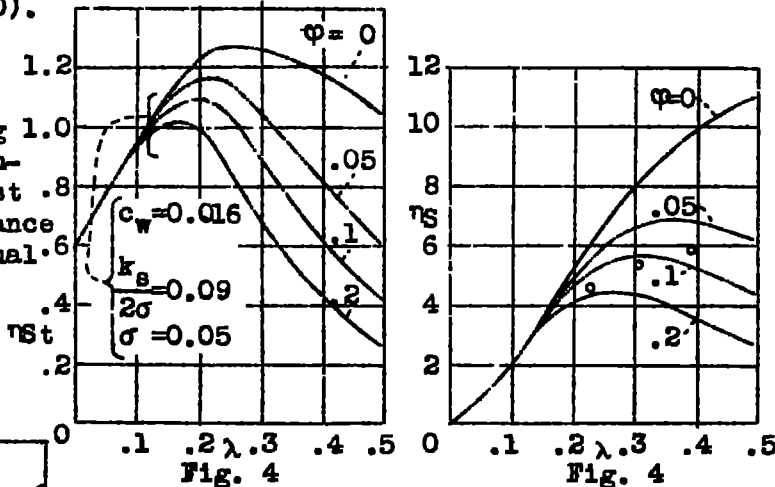


Fig. 5.- High-speed factor for constant blade loading $k_s/2\sigma = 0.072$, theory and experiment.

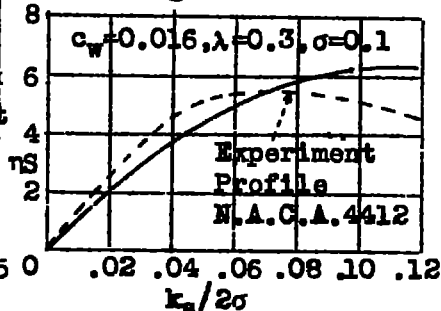


Fig. 6.-High-speed factor for constant coefficient of advance $\lambda = 0.3$, theory and experiment.

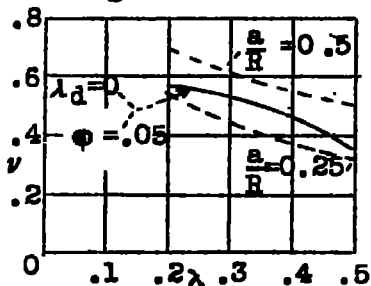


Fig. 7.-Performance ratio of helicopter screw performance to total performance against coefficient of advance λ .

NASA Technical Library



3 1176 01440 3522